Neuronal Excitability

Secondary Ammonium Agonists Make Dual Cation-π Interactions in $\alpha4\beta2$ Nicotinic Receptors

Michael R. Post,[1] Gabrielle S. Tender,[1] Henry A. Lester,[2] and Dennis A. Dougherty[1]

DOI:http://dx.doi.org/10.1523/ENEURO.0032-17.2017

[1]Division of Chemistry and Chemical Engineering, California Institute of Technology, Pasadena, CA 91125, and
[2]Division of Biology and Biological Engineering, California Institute of Technology, Pasadena, CA 91125

Abstract

A cation-π interaction between the ammonium group of an agonist and a conserved tryptophan termed TrpB is a near universal feature of agonist binding to nicotinic acetylcholine receptors (nAChRs). TrpB is one of five residues that form the aromatic box of the agonist binding site, and for the prototype agonists ACh and nicotine, only TrpB makes a functional cation-π interaction. We report that, in addition to TrpB, a significant cation-π interaction is made to a second aromatic, TyrC2, by the agonists metanicotine, TC299423, varenicline, and nornicotine. A common structural feature of these agonists, and a distinction from ACh and nicotine, is a protonated secondary amine that provides the cation for the cation-π interaction. These results indicate a distinction in binding modes between agonists with subtly different structures that may provide guidance for the development of subtype-selective agonists of nAChRs.

Key words: Parkinson's disease; Addiction; Ion channels; Nicotinic acetylcholine receptors; Electrophysiology; Non-canonical amino acids

Significance Statement

The $\alpha4\beta2$ nicotinic acetylcholine receptor (nAChR) binding site is made of several loops contributing five aromatic residues. Here, we show four secondary ammonium agonists, TC299423, metanicotine, varenicline, and nornicotine, make a cation-π interaction with TyrC2 in addition to the canonical cation-π interaction with TrpB. The prototypical agonists acetylcholine (a quaternary ammonium), and nicotine (a tertiary ammonium) only make a cation-π interaction with TrpB. This result indicates a new binding mode for agonists with only subtle structural differences and suggests that a more compact cation allows for greater interaction with loop C in the binding site.

Introduction

The neuronal nicotinic acetylcholine receptors (nAChRs) are members of the Cys-loop ligand-gated ion channel family and are established therapeutic targets for nicotine addiction, as well as possible targets for Parkinson's disease, Alzheimer's disease, pain, and other neural disorders (Romanelli et al., 2007). The receptors are pentamers, and 11 known subunits, $\alpha2$-7,9,10 and $\beta2$-4, combine to form distinct subtypes (Le Novère et al., 2002; Millar, 2003; Gotti et al., 2006; Zoli et al., 2015). The nAChR binding site lies at the extracellular α-β interface, and it contains an aromatic box motif that binds the cationic

Received January 26, 2017; accepted March 2, 2017; First published March 17, 2017.
The authors declare no competing financial interests.
Author contributions: M.R.P., G.S.T., H.A.L., and D.A.D. designed research; M.R.P. and G.S.T. performed research; M.R.P. and G.S.T. analyzed data; M.R.P. wrote the paper.
This work was supported by HHS | NIH | National Institute of Neurological Disorders and Stroke (NINDS) (100000065, Grant NS34407); HHS | NIH | National Institute on Drug Abuse (NIDA) (Funding 100000026, Grand DA 019375); and by Beckman Institute at Caltech. M.R.P. was supported by the NIH/NRSA Training Grant 5 T32 GM07616.

Correspondence should be addressed to Dennis A. Dougherty, California Institute of Technology, MC 164-30, 1200 East California Boulevard, Pasadena, CA 91125. E-mail: dadoc@caltech.edu.

DOI:http://dx.doi.org/10.1523/ENEURO.0032-17.2017

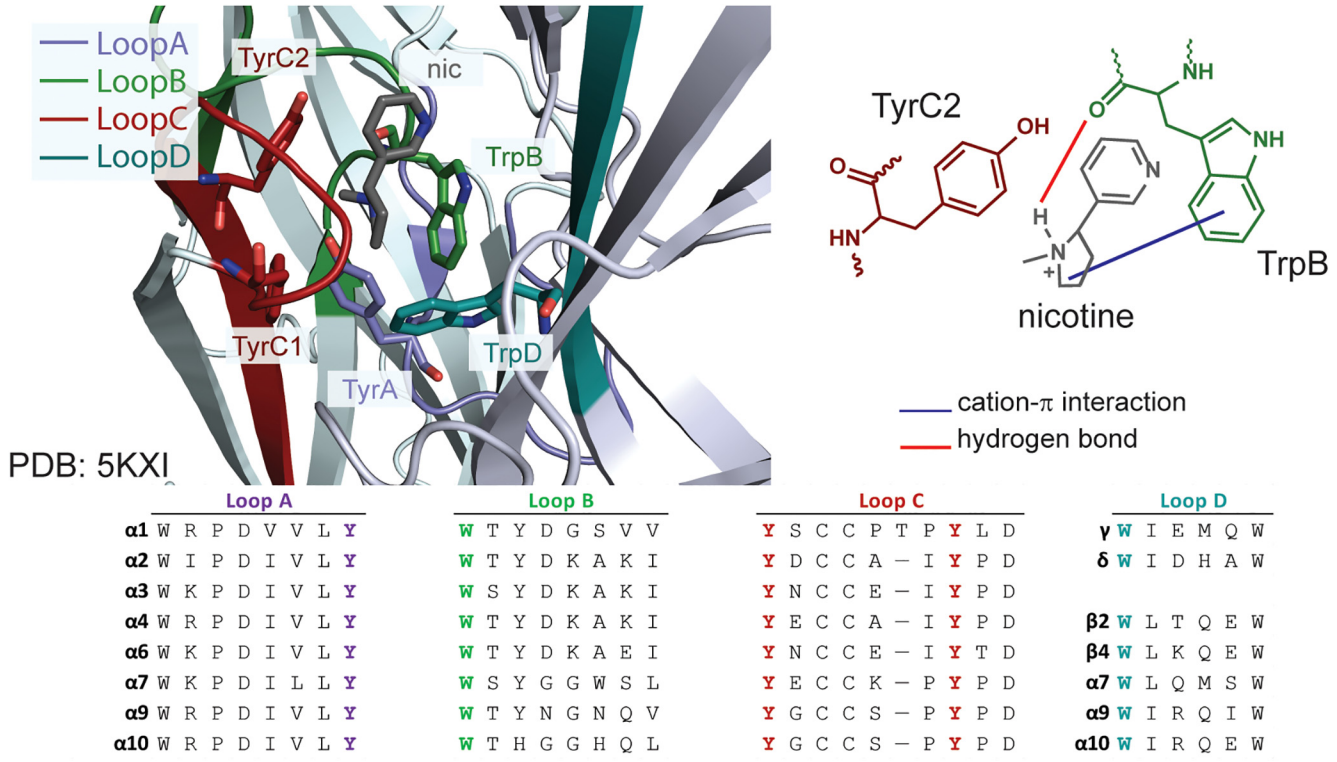

Figure 1. A view of nicotine at the $\alpha4\beta2$ binding site. The crystal structure of $\alpha4\beta2$ (PDB 5KXI) on the left shows the aromatic box motif, with each loop contributing to the binding site in a unique color and nicotine in gray. The schematic on the right details the hydrogen bond (red) and cation-π interaction (purple) interactions previously determined for nicotine with TrpB ($\alpha4$: 149), as well as how TyrC2 ($\alpha4$: 197) could interact with other agonists. TyrA ($\alpha4$: 93), TyrC1($\alpha4$: 190), and TrpD ($\beta2$: 57) are shown in the crystal structure but omitted from the schematic for clarity. An alignment of each loop contributing to the box in the human nAChR family is shown at the bottom.

moiety of the agonist through a cation-π interaction (Fig. 1; Dougherty, 1996, 2013; Van Arnam and Dougherty, 2014). Five aromatic residues are contributed by four loops, TyrA, Trp B, TyrC1, TyrC2, and TrpD (Corringer et al., 2000). In many studies of ligands binding to nAChRs, TrpB forms a functionally important cation-π interaction, while the other aromatics apparently play other roles (Xiu et al., 2009; Blum et al., 2010, 2013; Puskar et al., 2012; Tavares et al., 2012; Van Arnam and Dougherty, 2014).

A major goal in nAChR research is to develop agonists that target specific subtypes (Holladay et al., 1997; Quik and Wonnacott, 2011; Dineley et al., 2015). For example, the $\alpha4\beta2$-containing subtypes are expressed throughout the brain and are most associated with several aspects of nicotine addiction (De Biasi and Dani, 2011). The $\alpha6\beta2$-containing subtypes have a more restricted distribution. They occur on dopaminergic neurons, where they have been associated with reward-related behavior and Parkinson's disease, as well as on medial habenula neurons, which play a role in aversive behavior (Quik and McIntosh, 2006; Jackson et al., 2013; Henderson et al., 2014; Zuo et al., 2016). Finding agonists that meaningfully distinguish between the $\alpha4\beta2$ and $\alpha6\beta2$ interfaces is an unsolved challenge, but metanicotine (rivanicline, TC-2403, or RJR-2403) and TC299423 have been found to preferentially activate $\alpha4\beta2$- and $\alpha6\beta2$-containing subtypes, respectively (Drenan et al., 2008; Grady et al., 2010; Xiao et al., 2011; Wall, 2015).

Previous analysis of TC299423 at $\alpha6\beta2$ showed an unusual binding pattern, in that the agonist does not make a functional cation-π interaction with TrpB or any other aromatic box residue (Post et al., 2015); thus, a unique binding mode may contribute to its subtype selectivity. Here, TC299423 and other agonists were studied at the more extensively characterized $\alpha4\beta2$ receptor to see whether the unusual binding pattern persists. Several agonists were found to make cation-π interactions with both TrpB and TyrC2, and we show that this dual cation-π feature is a more general trend among secondary ammonium agonists (Fig. 2) at $\alpha4\beta2$.

Materials and Methods

Molecular biology

Rat $\alpha4$ and $\beta2$ subunits were used as the basis for the constructs. The L9'A mutation in the $\alpha4$ M2 transmembrane domain, at the gate of the channel, was incorporated to amplify signal by shifting the stability of the channel partially toward the active state. This $\alpha4$L'A$\beta2$ construct is described as wild type and/or $\alpha4\beta2$ throughout the report for clarity in comparing noncanonical mutations made to the binding site, which is over 60 Å away from the channel gate. All constructs were in the pGEMhe vector, a cDNA plasmid optimized for protein expression in *Xenopus* oocytes. Site-directed mutagenesis was performed by PCR

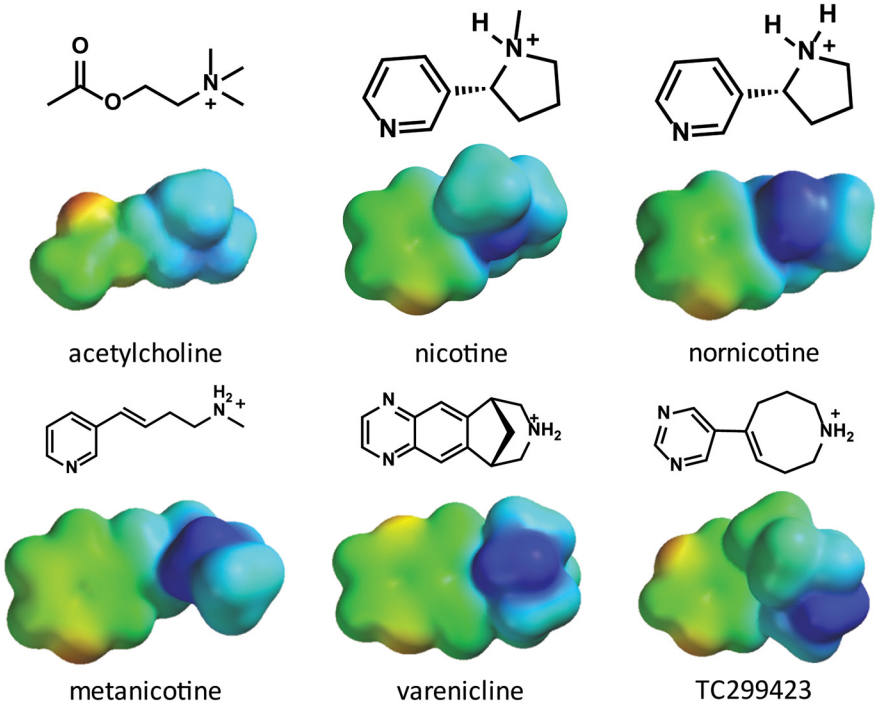

Figure 2. The structures and electrostatic potential maps of acetylcholine and nicotine are shown here for comparison to the secondary amine agonists and have been calculated with Hartree Fock 6-31G** (shown on a scale of −10, red and more negative electrostatic potential, to +150, blue and more positive electrostatic potential, kcal/mol).

using the Stratagene QuikChange protocol, and primers ordered from Integrated DNA Technologies. Circular cDNA was linearized with SbfI (New England Biolabs) and then transcribed *in vitro* using T7 mMessage mMachine kit (Life Technologies), with a purification step after each process (QIAGEN). Final concentrations were quantified by UV spectroscopy.

Ion channel expression

Xenopus laevis oocytes (stage V to VI) were sourced from both an institute facility and Ecocyte Bio Science. Oocytes were injected with 50-nL solution containing either 5- or 10-ng mRNA, injected in a 1:2 α4:β2 ratio to control for a pure population of the $(\alpha 4L9'A)_2(\beta 2)_3$ stoichiometry. The alternative stoichiometry $(\alpha 4)_3(\beta 2)_2$ has a much lower EC_{50} due to the extra L9'A mutation. We therefore avoided a mixed population containing both stoichiometries. Cells were incubated 24-48 h at 18°C in ND96 solution (96 mM NaCl, 2mM KCl, 1 mM $MgCl_2$, and 5mM HEPES, pH 7.5) enriched with theophylline, sodium pyruvate, and gentamycin.

Noncanonical amino acid incorporation

The cyanomethylester form of nitroveratryloxycarbonyl (NVOC)-protected tryptophan and phenylalanine analogues was coupled to dinucleotide dCA and enzymatically ligated to UAG-suppressor 74-mer THG73 $tRNA_{CUA}$. The product was verified by Matrix-assisted laser desorption/ionization (MALDI) time-of-flight mass spectrometry on a 3-hydroxypicolinic acid matrix. The noncanonical amino acid-coupled tRNA was deprotected by photolysis either on a 500 W Hg/Xe arc lam, filtered with Schott WG-320 and UG-11 filters, or with an M365LP1 365 nm 1150 mW LED lamp (Thor Labs) immediately before coinjection with mRNA containing the UAG mutation at the site of interest. mRNA and tRNA were typically injected in a 1:1 or 1:2 volume ratio in a total volume of 50 or 75 nL, respectively, so that 25 ng of mRNA was injected per cell. In cases where observed agonist-induced currents were low after 48-h incubation, likely due to low protein expression, a second injection of mRNA and tRNA was performed after 24 h. The fidelity of noncanonical amino acid incorporation was confirmed at Trp with a wild-type recovery experiment where tryptophan was loaded onto tRNA. If this experiment yielded similar to EC_{50} to wild type, then the cell incorporated the charged residue and nothing else. This was accomplished with the Tyr sites by comparing tRNA charged with Phe to a conventional Tyr-Phe mutation. A read-through/reaminoacylation test served as a negative control by injecting unacylated full-length 76-mer tRNA. Lack of current proved no detectable reaminoacylation at the suppression site.

Whole-cell electrophysiological characterization

(S)-nornicotine hydrochloride was purchased from Matrix Scientific, while varenicline (Pfizer), metanicotine, and TC299423 (Targacept) were generous gifts. Agonist-induced currents were recorded in TEVC mode using the OpusXpress 6000A (Molecular Devices) at a holding potential of −60 mV in a running buffer of Ca^{2+}-free ND96, which since $\alpha 4\beta 2$ is Ca^{2+} permeable, prevents interference from Ca^{2+}-activated channels endogenous to the oocyte. Agonists were prepared in Ca^{2+}-free ND96 and delivered to cells via a 1-mL application over 15 s followed by a 2-min

Table 1: TC299423

TrpB	EC_{50} (μM)	n_H	I_{max} (μA)	Fold shift	*N*
Trp	0.023 ± 0.0009	1.4 ± 0.06	0.22–1.46	1	15
F_1Trp	0.043 ± 0.0008	1.3 ± 0.03	0.12–1.2	1.8	11
F_2Trp	0.052 ± 0.001	1.2 ± 0.04	0.05–0.62	2.2	14
F_3Trp	0.13 ± 0.003	1.2 ± 0.03	0.11–1.41	5.5	12
F_4Trp	0.15 ± 0.007	1.1 ± 0.05	0.15–0.77	6.6	14
TyrC2	EC_{50} (μM)	n_H	I_{max} (μA)	Fold shift	*N*
Phe	0.098 ± 0.003	1.1 ± 0.03	0.06–1.08	1	17
F_1Phe	0.14 ± 0.005	1.2 ± 0.04	0.05–0.38	1.5	12
F_2Phe	1.6 ± 0.07	1.3 ± 0.06	0.05–0.57	16	9
F_3Phe	3.0 ± 0.25	1.3 ± 0.11	0.07–0.18	30	7

wash. For data from dose-response experiments were normalized, averaged, and fit to the Hill equation using Kaleidagraph (Synergy Software). In data tables, *N* is the total number of oocytes analyzed, and cells from different frogs on at least two different days were used for each point. Fluorination plots are visualized here with Prism (GraphPad Software). EC_{50} and Hill coefficient errors are presented as SEM.

Results

Binding studies of TC299423 and metanicotine at $\alpha4\beta2$

All studies here used the previously described $(\alpha L9'A)_2(\beta2)_3$ receptor (Kuryatov et al., 2005; Nelson et al., 2003). TC299423 was first probed for cation-π interactions at TrpB and TyrC2 (TyrA, TyrC1, and TrpD have never been implicated in a cation-π interaction). In these experiments, the site of the aromatic residue of interest is mutated to a TAG stop codon. mRNA made *in vitro* is injected into *Xenopus* oocytes alongside a bioorthogonal $tRNA_{CUA}$ that has been chemically appended to the noncanonical amino acid of interest. To probe for an agonist cation-π interaction, a series of residues with electron-withdrawing groups that weaken the interaction is used. Typically, fluorotryptophans (F_nTrp) are used to probe Trp and fluorophenylalanines (F_nPhe) are used to probe Tyr (fluorinating tyrosine causes the phenol group to deprotonate at physiologic pH). The endpoints of the two series, F_4Trp and F_3Phe, are both thought to approximate a situation in which the dominant electrostatic component of the cation-π interaction has been completely removed, allowing a semiquantitative comparison of Trp and Tyr residues. Any change in binding is revealed by a changed EC_{50} value, monitored by two-electrode voltage clamp electrophysiology dose-response experiments. If the interaction is weakened by these substitutions, EC_{50} correspondingly increases. This change is visualized in so-called fluorination plots of the log of the fold-shift in EC_{50} against the calculated gas-phase cation-π interaction strength.

At TrpB, TC299423 showed an increase in EC_{50} with each additional fluorine substituent on the ring (Table 1), but the maximum fold-shift in EC_{50} observed at F_4Trp was only 6.6-fold. While this is a modest loss of function, ACh experiences a 66-fold loss of function at F_4Trp in $\alpha4\beta2$ (Xiu et al., 2009), there is nevertheless a linear trend in the fluorination plot (Fig. 3). Thus, it can be said that TC299423 makes a functional, if modest, cation-π interaction with TrpB in $\alpha4\beta2$.

TyrC2 was then probed for a cation-π interaction with TC299423 and showed an unexpected trend, with F_3Phe substitution resulting in a 30-fold increase in EC_{50}. When presented as a fluorination plot (Fig. 4), these results show a linear trend, showing that in addition to a cation-π interaction with TrpB, TC299423 makes a functional, and energetically more significant, cation-π interaction at TyrC2.

Metanicotine, an isomer of nicotine in which the pyrrolidine ring has been opened, has antinociceptive effects in mice and is more potent and efficacious than ACh at $\alpha4\beta2$ receptors (Damaj et al., 1999; Papke et al., 2000). When

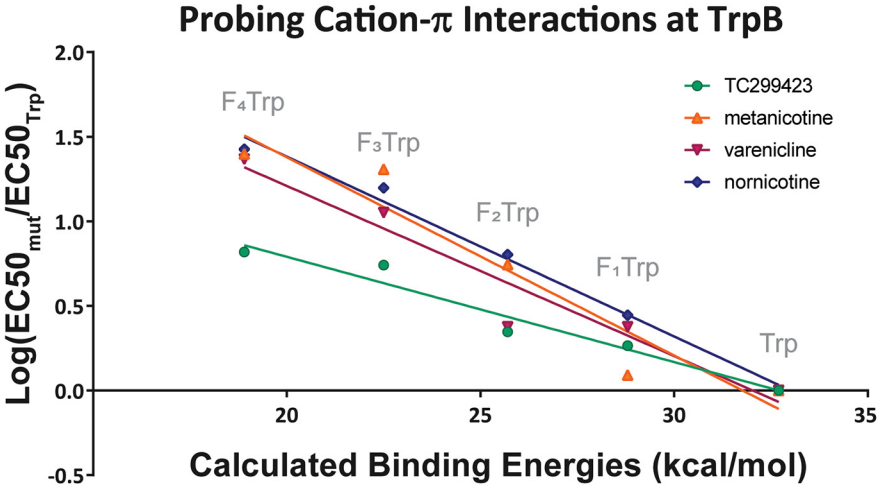

Figure 3. Fluorination plots of all the agonists tested in this report at TrpB in $\alpha4\beta2$. The *x*-axis is the predicted M06/6-31G(d,p) DFT-calculated energies between a sodium ion and each side chain (labeled) in the gas phase as described in Davis and Dougherty (2015). The *y*-axis is the log of the fold-shift in EC_{50}. Each agonist tested showed a linear trend and, therefore, demonstrated a functional cation-π interaction at TrpB, as previously seen with acetylcholine and nicotine. Data plotted for varenicline are from Tavares et al. (2012).

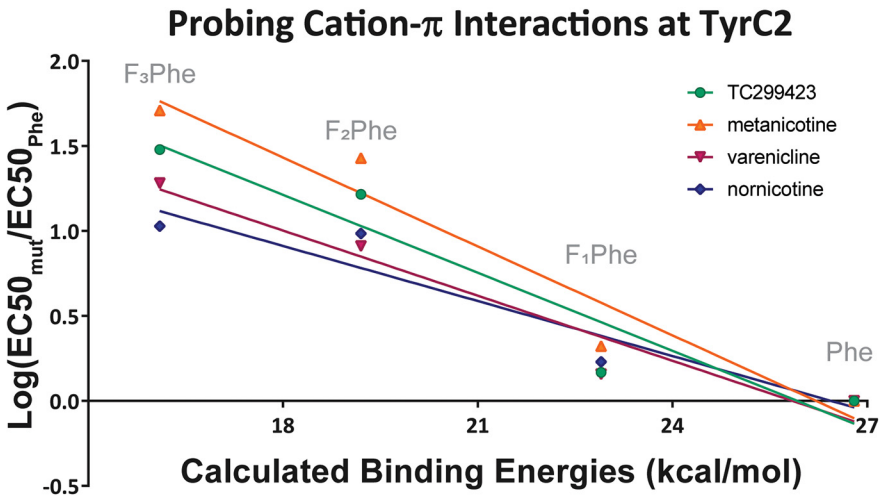

Figure 4. Fluorination plots of all the agonists tested in this report at TyrC2 in $\alpha4\beta2$. The *x*-axis is the predicted M06/6-31G(d,p) DFT-calculated energies between a sodium ion and each side chain (labeled) in the gas phase as described in Davis and Dougherty (2015). The *y*-axis is the log of the fold-shift in EC_{50}. Each agonist tested shows a linear trend and, therefore, demonstrates a functional cation-π interaction with TyrC2, a result not previously seen with acetylcholine or nicotine.

analyzed via a fluorination series at TrpB in $\alpha4\beta2$, metanicotine displayed a functional cation-π interaction, with a linear fluorination plot and F_4Trp resulting in a 25-fold shift in EC_{50} (Table 2; Fig. 3). TyrC2 also shows a linear fluorination plot, with the F_3Phe mutation causing a 51-fold shift relative to Phe (Fig. 4). TyrA was probed and showed no meaningful changes in metanicotine EC_{50} on fluorination (Table 2; nicotine and ACh also showed no meaningful shifts in EC_{50} at this site; Xiu et al., 2009). Thus, metanicotine also forms dual, functional cation-π interactions at TrpB and TyrC2 in $\alpha4\beta2$.

Both metanicotine and TC299423 are typical nicotinic pharmacophores in that they have a cationic amine moiety, a hydrogen bond donor associated with that amine, and a hydrogen bond acceptor several angstroms away (Blum et al., 2010). In contrast to the tertiary ammonium nicotine and the quaternary ammonium ACh, metanicotine and TC299423 are both secondary ammonium ions. Thus, to test whether this feature was associated with the novel dual cation-π interaction, additional secondary amine agonists were analyzed.

Establishing a binding trend for secondary amines

Varenicline (Chantix) is a smoking cessation drug that is thought to work by serving as a partial agonist to $\alpha4\beta2$ (Coe et al., 2005a, 2005b) It has a secondary ammonium

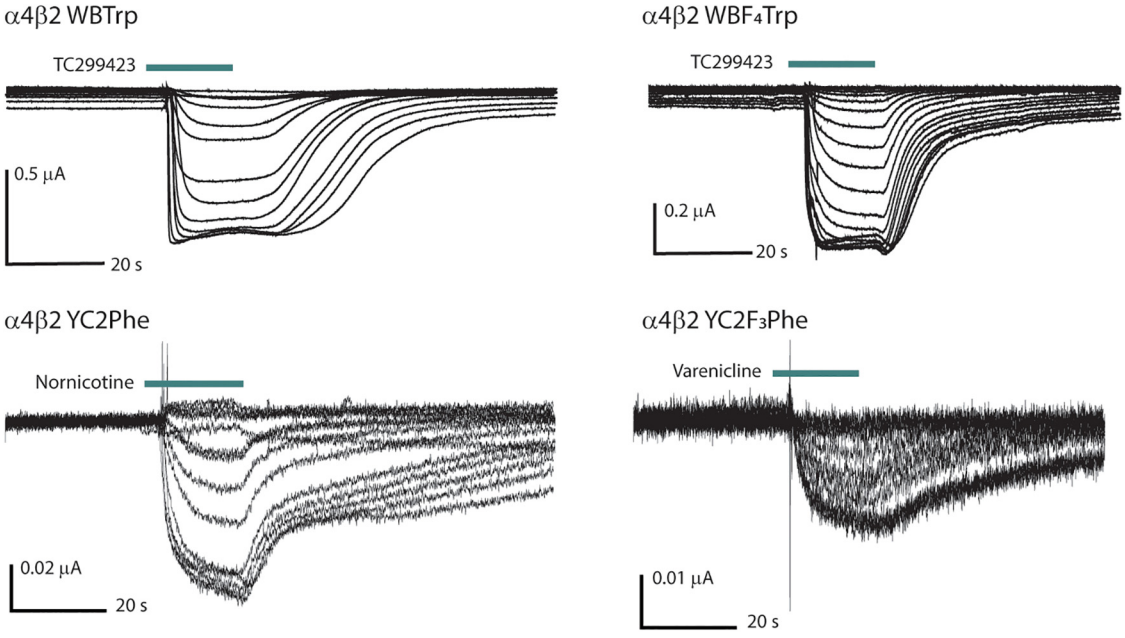

Figure 5. Representative traces from dose-response experiments with a variety of agonists, noncanonical amino acid substitutions, and I_{max} values.

Table 2: Metanicotine

TrpB	EC_{50} (μM)	n_H	I_{max} (μA)	Fold shift	*N*
Trp	0.64 ± 0.02	1.3 ± 0.0	0.08–0.89	1	13
F_1Trp	0.79 ± 0.02	1.4 ± 0.0	0.12–0.80	1.2	16
F_2Trp	3.6 ± 0.1	1.5 ± 0.1	0.15–0.56	5.6	14
F_3Trp	13 ± 1	1.6 ± 0.1	0.07–0.30	20	12
F_4Trp	16 ± 2	1.3 ± 0.1	0.03–0.11	25	12
TyrA	EC_{50} (μM)	n_H	I_{max} (μA)	Fold shift	*N*
Phe	19 ± 5	1.1 ± 0.2	0.02–0.16	1	7
F_3Phe	17 ± 2	1.3 ± 0.1	0.01–0.03	0.9	6
TyrC2	EC_{50} (μM)	n_H	I_{max} (μA)	Fold shift	*N*
Phe	0.41 ± 0.03	1.2 ± 0.07	0.06–2.78	1	17
F_1Phe	0.86 ± 0.06	1.2 ± 0.08	0.04–0.07	2.1	11
F_2Phe	11 ± 1	0.6 ± 0.1	0.03–0.13	27	8
F_3Phe	21 ± 1	1.4 ± 0.2	0.04–0.24	51	12

as its cationic center. This drug has previously been shown to form a cation-π interaction at TrpB in $\alpha4\beta2$ (Tavares et al., 2012), with a 23-fold shift in EC_{50} at F_4Trp (Table 3; Fig. 3), but had not been analyzed at TyrC2.

Nonsense-suppression-based fluorination studies were conducted for varenicline at TyrC2 as discussed above. The corresponding fluorination plot shows a linear trend with a 19-fold shift for F_3Phe, confirming that varenicline makes a cation-π interaction with TyrC2 in $\alpha4\beta2$ (Table 3; Fig. 4).

Varenicline was the third secondary ammonium agonist to demonstrate functional cation-π interactions with both TrpB and TyrC2 in $\alpha4\beta2$. To support the notion that a dual cation-π interaction is associated with secondary ammonium agonists in $\alpha4\beta2$, we transformed nicotine, which makes a single cation-π interaction at TrpB, into a secondary ammonium. Nornicotine, nicotine that has been demethylated at the pyrrolidine N, is a natural component of tobacco that is a precursor to the well-documented carcinogen *N*'-nitrosonicotine that is a by-product of the curing process.(Siminszky et al., 2005)

Nornicotine is much less potent than its methylated analog, with an EC_{50} of 1.8 μM, a 20-fold greater value than for nicotine. This agonist also elicits much smaller currents; however, the waveform shapes (Fig. 5) are consistent with other agonists, and a clear dose-response relation is present. The fluorination plot of nornicotine at TrpB shows a cation-π interaction, with F_4Trp resulting in a 27-fold shift in EC_{50}, demonstrating a functionally important cation-π interaction (Table 4; Fig. 3). Results at TyrC2 show the same type of trend seen for other secondary ammonium agonists analyzed in this report, with a linear fluorination plot and a 11-fold loss of function for F_3Phe (Table 4; Fig. 4).

Table 3: Varenicline

TrpB*	EC_{50} (μM)	n_H	Fold shift	*N*
Trp	0.0024 ± 0.0001	1.2 ± 0.1	1	15
F_1Trp	0.0057 ± 0.0002	1.2 ± 0.1	2.4	11
F_2Trp	0.0057 ± 0.0021	1.2 ± 0.1	2.4	14
F_3Trp	0.027 ± 0.001	1.3 ± 0.1	11	12
F_4Trp	0.056 ± 0.005	1.1 ± 0.1	23	14

TyrC2	EC_{50} (μM)	n_H	I_{max} (μA)	Fold shift	*N*
Phe	0.0014 ± 0.0002	1.3 ± 0.14	0.04–0.14	1	10
F_1Phe	0.0020 ± 0.00009	1.5 ± 0.09	0.02–0.08	1.4	8
F_2Phe	0.011 ± 0.00097	1.2 ± 0.11	0.02–0.1	8.1	12
F_3Phe	0.027 ± 0.0016	1.1 ± 0.06	0.02–0.09	19	8

Table 4: Nornicotine

TrpB	EC_{50} (μM)	n_H	I_{max} (μA)	Fold shift	*N*
Trp	1.7 ± 0.1	1.3 ± 0.1	1.33–9.37	1	13
F_1Trp	4.6 ± 0.2	1.3 ± 0.1	0.27–0.9	2.8	16
F_2Trp	11 ± 0.7	1.3 ± 0.1	0.04–0.11	6.4	8
F_3Trp	26 ± 2	1.5 ± 0.1	0.05–1.28	16	16
F_4Trp	44 ± 4	1.2 ± 0.1	0.95–1.51	27	8
TyrC2	EC_{50} (μM)	n_H	I_{max} (μA)	Fold shift	*N*
Phe	3.3 ± 0.3	1.2 ± 0.1	0.02–1.42	1	15
F_1Phe	5.5 ± 0.3	1.0 ± 0.1	0.04–0.11	1.7	11
F_2Phe	31 ± 3	1.2 ± 0.1	0.03–0.26	9.6	10
F_3Phe	35 ± 2	1.4 ± 0.1	0.02–0.14	11	12

Discussion

Structure-function studies of four different agonists with distinct overall structures but a common secondary ammonium moiety have established a functional cation-π interaction with both TrpB and TyrC2 in $\alpha4\beta2$ nAChRs. Nornicotine forms a cation-π interaction with TyrC2, but nicotine, which only differs from nornicotine by being a tertiary rather than secondary ammonium, does not. This nicotine/nornicotine comparison in particular presents a compelling case that the dual cation-π interaction is a consequence of the secondary ammonium group of select agonists at $\alpha4\beta2$.

The significance of TrpB in agonist binding to nAChRs remains a central tenet of the pharmacology of this system. In a cation-π interaction, the aromatic ring of Trp is a stronger binding site that those of Tyr or Phe, regardless of the nature of the cation, but Tyr and Phe can certainly make strong cation-π interactions (Davis and Dougherty, 2015). Early studies focused on ACh and nicotine and found that only TrpB showed a strong response to fluorination. We have now found that four other agonists show, in addition to TrpB, a significant response to fluorination at TyrC2. These four are structurally diverse but share a common feature of being a secondary ammonium. The implication is clear that the more compact secondary ammonium is able to establish an additional interaction compared with the bulkier quaternary (ACh) or tertiary (nicotine) systems.

Two studies of the primary ammonium agonist GABA at pentameric receptors, one at the RDL insect GABA receptor and one at the prokaryotic *Erwinia* ligand-gated ion channel (ELIC) receptor, show that this primary ammonium agonist makes functionally important cation-π interactions to the aromatics at positions B and C2 (Lummis et al., 2005; Spurny et al., 2012). Again, a more compact agonist can make a dual cation-π interaction. A recent computational study of the AChBP aromatic box suggests that the side chains of each aromatic box residue can contribute to the overall cation-π binding energy in the ACh-AChBP complex (Davis and Dougherty, 2015). However, from a functional perspective, only TrpB is univer-

sally important, with TyrC2 being identified here as contributing in some, but not all, cases.

A popular model for nAChR gating proposes that loop C moves on agonist binding so as to clamp down on the agonist and more clearly define the aromatic box (Wang et al., 2009). This movement of loop C is proposed to be a key functional feature of the gating mechanism. It may be that with the less bulky secondary ammonium agonists, loop C is able to move closer to the agonist. This larger motion by loop C leads to a closer contact between TyrC2 and the agonist, enabling a cation-π interaction and making TyrC2 responsive to fluorination. AChBP structures with varenicline versus nicotine bound do not show a meaningful difference in the position of loop C, but AChBP did not evolve to undergo a gating process and likely undergoes minimal conformational changes when binding small molecules (Celie et al., 2004; Rucktooa et al., 2012).

In summary, we have found a distinction in the binding mode of agonists at the $\alpha4\beta2$ nAChR. The natural agonist ACh and the prominent component of tobacco nicotine both make a cation-π interaction to TrpB, along with other hydrogen bonding interactions. In contrast, four agonists that share a common feature of being secondary ammonium ions make a dual cation-π interaction to TrpB and TyrC2. This pattern may be unique to the $\alpha4\beta2$ subtype, as it was not reported for TC299423 at the $\alpha6\beta2$ subtype (Post et al., 2015). Further studies of other agonists and other subtypes could provide valuable guidance in designing more subtype-selective activators of nAChRs.

References

Blum AP, Arnam EBV, German LA, Lester HA, Dougherty DA (2013) Binding interactions with the complementary subunit of nicotinic receptors. J Biol Chem 288:6991–6997. CrossRef

Blum AP, Lester HA, Dougherty DA (2010) Nicotinic pharmacophore: the pyridine N of nicotine and carbonyl of acetylcholine hydrogen bond across a subunit interface to a backbone NH. Proc Natl Acad Sci USA 107:13206–13211. CrossRef

Celie PHN, van Rossum-Fikkert SE, van Dijk WJ, Brejc K, Smit AB, Sixma TK (2004) Nicotine and carbamylcholine binding to nicotinic acetylcholine receptors as studied in AChBP crystal structures. Neuron 41:907–914. CrossRef

Coe JW, Brooks PR, Vetelino MG, Wirtz MC, Arnold EP, Huang J, Sands SB, Davis TI, Lebel LA, Fox CB, Shrikhande A, Heym JH, Schaeffer E, Rollema H, Lu Y, Mansbach RS, Chambers LK, Rovetti CC, Schulz DW, Tingley FD 3rd, et al. (2005a) Varenicline: an $\alpha4\beta2$ nicotinic receptor partial agonist for smoking cessation. J Med Chem 48:3474–3477.

Coe JW, Brooks PR, Wirtz MC, Bashore CG, Bianco KE, Vetelino MG, Arnold EP, Lebel LA, Fox CB (2005b) 3,5-Bicyclic aryl piperidines: a novel class of alpha4beta2 neuronal nicotinic receptor partial agonists for smoking cessation. Bioorg Med Chem Lett 15:4889–4897. CrossRef

Corringer P-J, Novère NL, Changeux J-P (2000) Nicotinic receptors at the amino acid level. Annu Rev Pharmacol Toxicol 40:431–458. CrossRef Medline

Damaj MI, Glassco W, Aceto MD, Martin BR (1999) Antinociceptive and pharmacological effects of metanicotine, a selective nicotinic agonist. J Pharmacol Exp Ther 291:390–398. Medline

Davis MR, Dougherty DA (2015) Cation–π interactions: computational analyses of the aromatic box motif and the fluorination strategy for experimental evaluation. Phys Chem Chem Phys 17:29262–29270. CrossRef

De Biasi M, Dani JA (2011) Reward, addiction, withdrawal to nicotine. Annu Rev Neurosci 34:105–130. CrossRef Medline

Dineley KT, Pandya AA, Yakel JL (2015) Nicotinic ACh receptors as therapeutic targets in CNS disorders. Trends Pharmacol Sci 36:96–108. CrossRef Medline

Dougherty DA (1996) Cation-π interactions in chemistry and biology: a new view of benzene, Phe, Tyr, and Trp. Science 271:163–168. Medline

Dougherty DA (2013) The cation$-\pi$ interaction. Acc Chem Res 46:885–893. CrossRef Medline

Drenan RM, Grady SR, Whiteaker P, McClure-Begley T, McKinney S, Miwa JM, Bupp S, Heintz N, McIntosh JM, Bencherif M, Marks MJ, Lester HA (2008) In vivo activation of midbrain dopamine neurons via sensitized, high-affinity $\alpha6^*$ nicotinic acetylcholine receptors. Neuron 60:123–136. CrossRef

Gotti C, Zoli M, Clementi F (2006) Brain nicotinic acetylcholine receptors: native subtypes and their relevance. Trends Pharmacol Sci 27:482–491. CrossRef

Grady SR, Drenan RM, Breining SR, Yohannes D, Wageman CR, Fedorov NB, McKinney S, Whiteaker P, Bencherif M, Lester HA, Marks MJ (2010) Structural differences determine the relative selectivity of nicotinic compounds for native $\alpha4\beta2^*$-, $\alpha6\beta2^*$-, $\alpha3\beta4^*$- and $\alpha7$-nicotine acetylcholine receptors. Neuropharmacology 58:1054–1066. CrossRef

Henderson BJ, Srinivasan R, Nichols WA, Dilworth CN, Gutierrez DF, Mackey EDW, McKinney S, Drenan RM, Richards CI, Lester HA (2014) Nicotine exploits a COPI-mediated process for chaperone-mediated up-regulation of its receptors. J Gen Physiol 143:51–66. CrossRef

Holladay MW, Dart MJ, Lynch JK (1997) Neuronal nicotinic acetylcholine receptors as targets for drug discovery. J Med Chem 40:4169–4194. CrossRef Medline

Jackson KJ, Sanjakdar SS, Muldoon PP, McIntosh JM, Damaj MI (2013) The $\alpha3\beta4^*$ nicotinic acetylcholine receptor subtype mediates nicotine reward and physical nicotine withdrawal signs independently of the $\alpha5$ subunit in the mouse. Neuropharmacology 70:228–235. CrossRef

Kuryatov A, Luo J, Cooper J, Lindstrom J (2005) Nicotine acts as a pharmacological chaperone to up-regulate human $\alpha4\beta2$ acetylcholine receptors. Mol Pharmacol 68:1839–1851. CrossRef Medline

Le Novère N, Corringer PJ, Changeux JP (2002) The diversity of subunit composition in nAChRs: evolutionary origins, physiologic and pharmacologic consequences. J Neurobiol 53:447–456. CrossRef

Lummis SCR, L. Beene D, Harrison NJ, Lester HA, Dougherty DA (2005) A cation-π binding interaction with a tyrosine in the binding site of the $GABA_C$ receptor. Chem Biol 12:993–997. CrossRef

Millar NS (2003) Assembly and subunit diversity of nicotinic acetylcholine receptors. Biochem Soc Trans 31:869–874. CrossRef Medline

Nelson ME, Kuryatov A, Choi CH, Zhou Y, Lindstrom J (2003) Alternate stoichiometries of $\alpha4\beta2$ nicotinic acetylcholine receptors. Mol Pharmacol 63:332–341. Medline

Papke RL, Webster JC, Lippiello PM, Bencherif M, Francis MM (2000) The activation and inhibition of human nicotinic acetylcholine receptor by RJR-2403 indicate a selectivity for the $\alpha4\beta2$ receptor subtype. J Neurochem 75:204–216. CrossRef

Post MR, Limapichat W, Lester HA, Dougherty DA (2015) Heterologous expression and nonsense suppression provide insights into agonist behavior at $\alpha6\beta2$ nicotinic acetylcholine receptors. Neuropharmacology 97:376–382. CrossRef

Puskar NL, Lester HA, Dougherty DA (2012) Probing the effects of residues located outside the agonist binding site on drug-receptor selectivity in the nicotinic receptor. ACS Chem Biol 7:841–846. CrossRef

Quik M, McIntosh JM (2006) Striatal $\alpha6^*$ nicotinic acetylcholine receptors: potential targets for Parkinson's disease therapy. J Pharmacol Exp Ther 316:481–489. CrossRef

Quik M, Wonnacott S (2011) $\alpha6\beta2^*$ and $\alpha4\beta2^*$ nicotinic acetylcholine receptors as drug targets for Parkinson's disease. Pharmacol Rev 63:938–966. CrossRef Medline

Romanelli MN, Gratteri P, Guandalini L, Martini E, Bonaccini C, Gualtieri F (2007) Central nicotinic receptors: structure, function, ligands, and therapeutic potential. ChemMedChem 2:746–767. CrossRef

Rucktooa P, Haseler CA, van Elk R, Smit AB, Gallagher T, Sixma TK (2012) Structural characterization of binding mode of smoking cessation drugs to nicotinic acetylcholine receptors through study of ligand complexes with acetylcholine-binding protein. J Biol Chem 287:23283–23293. CrossRef

Siminszky B, Gavilano L, Bowen SW, Dewey RE (2005) Conversion of nicotine to nornicotine in *Nicotiana tabacum* is mediated by CYP82E4, a cytochrome P450 monooxygenase. Proc Natl Acad Sci USA 102:14919–14924. CrossRef Medline

Spurny R, Ramerstorfer J, Price K, Brams M, Ernst M, Nury H, Verheij M, Legrand P, Bertrand D, Bertrand S, Dougherty DA, de Esch IJ, Corringer PJ, Sieghart W, Lummis SC, Ulens C (2012) Pentameric ligand-gated ion channel ELIC is activated by GABA and modulated by benzodiazepines. Proc Natl Acad Sci USA 109:E3028–E3034. CrossRef Medline

Tavares XDS, Blum AP, Nakamura DT, Puskar NL, Shanata JAP, Lester HA, Dougherty DA (2012) Variations in binding among several agonists at two stoichiometries of the neuronal, $\alpha4\beta2$ nicotinic receptor. J Am Chem Soc 134:11474–11480. CrossRef

Van Arnam EB, Dougherty DA (2014) Functional probes of drug–receptor interactions implicated by structural studies: Cys-loop receptors provide a fertile testing ground. J Med Chem 57:6289–6300. CrossRef

Wall TR (2015). Effects of TI-299423 on neuronal nicotinic acetylcholine receptors. Pasadena: California Institute of Technology.

Wang H-L, Toghraee R, Papke D, Cheng X-L, McCammon JA, Ravaioli U, Sine SM (2009) Single-channel current through nicotinic receptor produced by closure of binding site C-loop. Biophys J 96:3582–3590. CrossRef

Xiao C, Srinivasan R, Drenan RM, Mackey EDW, McIntosh JM, Lester HA (2011) Characterizing functional $\alpha6\beta2$ nicotinic acetylcholine receptors in vitro: mutant $\beta2$ subunits improve membrane expression, and fluorescent proteins reveal responsive cells. Biochem Pharmacol 82:852–861. CrossRef

Xiu X, Puskar NL, Shanata JAP, Lester HA, Dougherty DA (2009) Nicotine binding to brain receptors requires a strong cation–π interaction. Nature 458:534–537. CrossRef

Zoli M, Pistillo F, Gotti C (2015) Diversity of native nicotinic receptor subtypes in mammalian brain. Neuropharmacology 96:302–311. CrossRef Medline

Zuo W, Xiao C, Gao M, Hopf FW, Krnjević K, McIntosh JM, Fu R, Wu J, Bekker A, Ye J-H (2016) Nicotine regulates activity of lateral habenula neurons via presynaptic and postsynaptic mechanisms. Sci Rep 6:32937. CrossRef